



## Use of *Paliurus spina-christi* Mill. as a novel biosorbent: efficient biosorption of Pb(II) and Cd(II) ions from aqueous solution

Ferda Özmal<sup>a,\*</sup>, Melike Kale<sup>a</sup>, Çiğdem Ay<sup>b</sup>

<sup>a</sup>Department of Biochemistry, Science and Art Faculty, Kütahya Dumlupınar University, Kütahya, Turkey, Tel. +90 274 2652051/3343; emails: ferda.ozmal@dpu.edu.tr (F. Özmal), gpmelike@hotmail.com (M. Kale)

<sup>b</sup>Department of Chemistry, Science and Art Faculty, Kütahya Dumlupınar University, Kütahya, Turkey, email: cigdem.ay@dpu.edu.tr

Received 16 September 2021; Accepted 5 January 2022

### ABSTRACT

The biosorption process of lead(II) and cadmium(II) ions onto blackthorn (*Paliurus spina-christi* Mill.) was clarified by characterizing the biosorbent with Fourier-transform infrared spectroscopy, scanning electron microscopy and energy-dispersive X-ray analyses. The effect of pH, biosorbent dosage, contact time and temperature on the biosorption yield was studied. There was an increased tendency for biosorption with increasing temperature for both metals, and the best biosorption capacity was measured at 40°C. The highest biosorption capacity was obtained with a biosorbent dosage of 2.0 g L<sup>-1</sup> at pH 5.5 for Pb(II) ions and 6.0 g L<sup>-1</sup> biosorbent dosage at pH 5.0 for Cd(II) ions. Biosorption equilibrium was approached within 50 min for Pb(II) ions and 60 min for Cd(II) ions. The Langmuir isotherm model was found to be the best, with the maximum monolayer biosorption capacity of 231.7 and 36.84 mg g<sup>-1</sup> for Pb(II) and Cd(II) ions, respectively. For both metals, the pseudo-second-order kinetic model was determined to be applicable. Furthermore, the desorption ability of biosorbent is investigated through consecutive biosorption–desorption cycles. After the third cycle, desorption yield decreased to 87% and 63% for Pb(II) and Cd(II) ions. The real sample application is performed by preparing simulated wastewater. The results showed that while the Pb(II) removal was not affected by the medium matrix, Cd(II) removal depends on the co-existing ions. Overall, our study provides a practical approach for the removal of Pb(II) and Cd(II) ions from the contaminated aquatic media.

**Keywords:** Biosorption; Cadmium; Isotherms; Kinetics; Lead; *Paliurus spina-christi* Mill.

### 1. Introduction

Water pollution is a serious problem, having large effects on human and animal health [1]. Chemical wastes resulting from industrial activities, rapid urbanization, the use of pesticides, increases in production and consumption are the underlying reasons for environmental problems associated with water contamination. Industrial effluents include primarily heavy metals and organics that are detrimental to the health of humans and other living organisms [2,3].

Because these pollutants are toxic, non-biodegradable, and carcinogenic, disposal of effluents prior to entering the food chain by way of joining the rivers and underground waters is essential for protecting the health of living organisms [4–6]. Traditional techniques applied to industrial wastewaters to remove heavy metals before discharge process are generally hydrogen peroxide treatment, membrane technologies, chemical precipitation, ion exchange, flotation, Fenton reagent, advanced oxidation processes, biological treatment, solvent extraction and adsorption [2,5,7,8]. These

\* Corresponding author.

effluent treatment methods have some disadvantages that include high costs, inadequate metal removal, huge sludge formations, need for chemical reagents and high energy requirements [5,9]. Additionally, mentioned methods can also include unsuitable operating conditions, making the biosorption process a favourite due to its eco-friendly nature, low operational costs, reusability, effective removal efficiency, and easy handling [10,11].

Various biological materials, both dead and living, are used as biosorbents. The mechanism of metal biosorption differs according to the status of biomass. There are two steps at the biosorption process by living cells. The first is one of or a combination of the following mechanisms: ion exchange, complex and chelate formation, adsorption, micro-precipitation [12] and the second is accumulation. In the first step, interactions between the metal ions and functional groups of the cell surface are the main subject. Metal ions bind to the active sites of structures on the cell wall such as proteins and polysaccharides. That is a passive process and generally, equilibrium is reached quickly in the process. For desorption, many eluting agents can be used. The second-step includes the active process. Metal ions pass through the cell wall and get into the cells of organisms. Biosorption process carried out by non-living biomass is controlled only by the passive mode independent from metabolism [13] and has many advantages according to active mode, including bioaccumulation. In the biosorption process by passive mode, biomass has no toxicity danger and need of nutrition. Besides, these biological-originated materials are low-cost sorbents and can be easily accessible from the environment directly or as agriculture and industry waste [13].

In recent years, researchers used agricultural by-products widely to remove heavy metals from wastewaters [1]. Marine and agriculture originated various shells, chitin, fruit pods, sawdust, compost, and leaves are some materials used for this purpose [1,5]. The metal uptake ability of biosorbents arises from the electrostatic attraction between metal cations and negatively charged chemical groups such as carboxyl, hydroxyl, phosphoryl, phosphate, sulfate, and the amino groups of their proteins, carbohydrates, and phenol compounds [12,14].

Lead is one of the most hazardous metals for human health. According to the Environmental Protection Agency (EPA), the permissible upper limit of lead in drinking water is  $0.05 \text{ mg L}^{-1}$ , and higher amounts of lead in water are known to be toxic [15,16]. The significant effects of lead (II) ion toxicity in humans occur in the kidney, liver, red blood cells, and nervous and reproductive systems. Anemia, hypertension, learning disabilities, kidney damage, mental retardation, and abortion are some of the adverse effects of lead uptake [17]. Cadmium is also toxic, similar to lead. Cadmium exposure leads to many health problems such as renal dysfunction, liver damage, lung insufficiency, high blood pressure, and bone lesions [18]. It is reported that cadmium causes these effects through the denaturation of nucleic acids, disruption of protein metabolism, and repression of cell division [19]. According to the World Health Organization (WHO), permissible cadmium concentrations in natural waters should be limited to  $0.001 \text{ mg L}^{-1}$  [20]. Biosorption seems to be a proper technique for removing both lead(II) and cadmium(II) ions at very dilute concentrations.

*Paliurus spina-christi* Mill. is commonly distributed in Turkey, Crimea, Southwest, South and Southeast Europe, Africa, the Balkans and the Caucasus. It grows spontaneously in forest areas, among bushes, in grassy, dry, stony places, and warm regions of Turkey. It spreads from sea level to an altitude of 1,400 m. It is 2–4 m tall, densely branched, thorny, growing with side shoots, and a scattered-topped plant. It blooms yellow and green in May-June, and flower bunches are in bulk. The fruit of this plant has been used for the treatment of several diseases for many years [21]. The leaf anatomy of *Paliurus spina-christi* is closely related to the species of the genus *Ziziphus* Mill. Most of the information that is generally available in the literature is about *Ziziphus* Mill. [22].

The main objective of this research is to determine the potential for lead(II) and cadmium(II) ion removal by blackthorn (*Paliurus spina-christi* Mill.) [23] from aqueous solutions in batch systems. The chosen biomass is an abundantly available agricultural material for which there is no knowledge about the biosorption ability from the literature. pH, biosorbent dosage, contact time, and temperature are the studied parameters. The Langmuir and Freundlich models were used to describe the equilibrium isotherms. The mechanism of biosorption of Pb(II) and Cd(II) ions onto the blackthorn (*Paliurus spina-christi* Mill.) was also clarified in terms of kinetics. To determine the applicability of proposed process to large-scale treatments, desorption studies and an application from simulated wastewater were performed.

## 2. Materials and methods

### 2.1. Biomass preparation

Blackthorn (*Paliurus spina-christi* Mill.) was used for the biosorption of Pb(II) and Cd(II) ions from aqueous solutions. Biomass samples were collected from the Gölpazarı District of the Bilecik Province in Turkey. The collected fruits were washed with ultrapure water and dried at room temperature. As a result of preliminary studies, it was decided to use the wing parts of the plant. The wings were milled and rewashed with ultrapure water. These were dried in an oven at  $80^\circ\text{C}$  for 48 h and sieved using a  $150 \mu\text{m}$  fraction. The under sieve material was dried again in the oven at  $80^\circ\text{C}$  for 2 h and then bottled. The biosorbent was thus made ready for use in all the experiments.

### 2.2. Chemicals and instrumentation

All chemicals used in the study were of analytical reagent grade.  $1,000 \text{ mg L}^{-1}$  Pb(II) ions solution and  $1,000 \text{ mg L}^{-1}$  Cd(II) ions solution were prepared as stock solutions using  $\text{Pb}(\text{NO}_3)_2$  and  $\text{Cd}(\text{NO}_3)_2$  salts from Merck (Germany). All dilutions were made from stock solutions for the desired concentrations. Ultrapure water from Milipore ultrapure system (Germany) was used in all experiments. HCl and NaOH solutions prepared from Merck (Germany) were used to adjust the pH with a WTW 720 series pH meter (Weilheim, Germany). Elemental analyses were carried out with a PinAAcle 900T Model (Perkin Elmer, USA) flame atomic absorption spectrometer (FAAS). Fourier-transform infrared spectroscopy (FT-IR)

(Bruker Alpha Platinum ATR, Germany) spectra of dried unloaded biosorbent and Pb(II)-loaded and Cd(II)-loaded biosorbent were evaluated in the range of 400–4,000  $\text{cm}^{-1}$  wavenumber to determine the functional groups at the surface of the biomass. The morphology of the biomass before and after the biosorption was identified using a scanning electron microscopy/energy-dispersive X-ray (SEM/EDX) (FEI Nova Nanosem 650, USA) analyses. Brunauer–Emmett–Teller (BET) surface area analysis of *Paliurus spina-christi* Mill. were determined using a surface area analyzer (Quantachrome Corporation, Autosorb-6) and zeta potential measurements of unloaded biosorbent; Pb(II) and Cd(II) ions loaded biosorbents were determined using a Zetasizer Nano Series Nano-ZS (Malvern Inst. Ltd., UK).

### 2.3. Biosorption experiments by batch procedure

Biosorption experiments were performed as a function of parameters that include pH, biosorbent dosage, contact time, and temperature. In order to study the effect of pH, 50 mL of 100  $\text{mg L}^{-1}$  Pb(II) ions and Cd(II) ions solutions were added onto 0.1 g of biomass samples, and the mixtures were stirred in the flasks at 500 rpm for 1 h at the pH interval of 1.5–6.0. Biosorbent dosage was varied between the 0.5–6.0  $\text{g L}^{-1}$  to indicate the influence of this parameter. 50 mL of 100  $\text{mg L}^{-1}$  Pb(II) ion and Cd(II) ion solutions were added to the different amounts of biosorbents at the optimum pH values and mixed for an hour at room temperature. Optimum values were obtained using pH of 5.5 and 5.0 and biosorbent dosage of 2.0 and 6.0  $\text{g L}^{-1}$  for Pb(II) and Cd(II) ions, respectively. These values were used as constants in the remaining experiments. Biosorption capacities of both ions were found using solutions in the range of 75–250  $\text{mg L}^{-1}$ . The results were evaluated by means of Langmuir and Freundlich isotherm models at 20°C, 30°C, and 40°C. Kinetics of the biosorption of Pb(II) and Cd(II) ions onto the biosorbent were also investigated using 50 mL of 100  $\text{mg L}^{-1}$  solutions at the constant pH and biosorbent dosage. The biosorbent was mixed with the solutions at time intervals between 5 and 180 min at various temperatures, from 20°C to 40°C.

When the biosorption reached equilibrium in all experiments, flask contents were filtered through filter paper, and the filtrates were analyzed for the residual metal ion concentration by FAAS. Experiments were repeated three times in all parameters, and the average values were used. Percentage of metal removal and biosorption capacity of *Paliurus spina-christi* Mill. were calculated from the following equations:

$$\text{Biosorption\%} = \frac{(C_i - C_e)}{C_i} \times 100 \quad (1)$$

$$q_e = \frac{V(C_i - C_e)}{m} \quad (2)$$

where  $q_e$  ( $\text{mg g}^{-1}$ ) is the biosorption capacity,  $C_i$  and  $C_e$  ( $\text{mg L}^{-1}$ ) are metal ions initial and equilibrium concentrations in the aqueous solution, respectively.  $m$  (g) is the weight of *Paliurus spina-christi* Mill.  $V$  (L) is the volume of the solution.

### 2.4. Desorption experiments

Desorption of Pb(II) and Cd(II) ions from the loaded biosorbents at optimized conditions (pH: 5.5 (Pb(II)), 5.0 (Cd(II)); biosorbent dosage: 2  $\text{g L}^{-1}$  (Pb(II)), 6  $\text{g L}^{-1}$  (Cd(II)); contact time: 60 min; metal concentrations: 100  $\text{mg L}^{-1}$ ; solution volume: 50 mL) were studied with 0.1 M HCl and  $\text{HNO}_3$ . After each biosorption cycle, the loaded biosorbents were filtered and dried. Then the loaded biosorbents were mixed with 50 mL of desorption agents at room temperature for 1 h.

### 2.5. Application in synthetic pollutants

The biosorption ability of blackthorn was also tested by an application in simulated wastewater to evaluate its capacity in the presence of other pollutants. The content of simulated wastewater was prepared according to the study reported by Ay et al. [24]. In brief, the simulated wastewater includes 100  $\text{mg L}^{-1}$  Pb(II) and Cd(II) ions along with many other components such as 0.25 g glucose, 0.15 g  $\text{KH}_2\text{PO}_4$ , 0.01 g  $\text{MgSO}_4 \cdot 7\text{H}_2\text{O}$ , 0.05 g  $\text{CaCl}_2 \cdot 2\text{H}_2\text{O}$ , 0.05 g  $\text{Na}_2\text{SO}_4$ , 0.10 g  $\text{Na}_2\text{CO}_3$ , 0.02 g  $\text{FeSO}_4 \cdot 7\text{H}_2\text{O}$ , 0.01 g  $\text{NiCl}_2 \cdot 6\text{H}_2\text{O}$ , 0.003 g  $\text{CuSO}_4 \cdot 5\text{H}_2\text{O}$ , 0.002 g  $\text{CoCl}_2 \cdot 6\text{H}_2\text{O}$ , and 0.015 g  $\text{ZnCl}_2$  in 250 mL of tap water. The study was performed at the optimum pH of 5.5 and biosorbent concentration of 2  $\text{g L}^{-1}$  for the removal of Pb(II) ions or pH of 5, and biosorbent concentration of 6  $\text{g L}^{-1}$  for the biosorption of Cd(II) ions. These certain amounts of biosorbents were added to 50 mL of pH adjusted wastewater and mixed for an hour at room temperature. After an hour, the remaining amount of Pb(II) and Cd(II) ions in the solution were determined by FAAS.

## 3. Results and discussions

### 3.1. Characterization of biosorbent

In previous studies, six flavonoid glycosides were isolated from *Paliurus spina-christi* Mill., which are used as traditional herbal medicine in diseases such as diarrhea and rheumatism [25,26]. Flavonoid is phenolic compounds consisting of fifteen carbon atoms and is commonly found in plants [27,28]; in addition to phenolic groups, they also contain C=O, C–O–C, C=C in their structures. The FT-IR spectra of unloaded biosorbent, Cd(II)-loaded, and Pb(II)-loaded biosorbents were evaluated in terms of the interactions between the metal ions (M) and the functional groups on the surface of the *Paliurus spina-christi* Mill. (Fig. 1). As can be seen in Fig. 1a, the broad stretching band at 3,330  $\text{cm}^{-1}$  represents the –OH groups as a functional group of carbohydrates, phenols, and flavonoids, previously reported by El-Ansary et al. [29]. The peak at 2,917  $\text{cm}^{-1}$  reveals the C–H vibration peaks connected to the aliphatic chain. The peaks observed at 1,608 and 1,318  $\text{cm}^{-1}$  belong to C=O stretching (carboxylic or amide) and C=C peaks [29,30], and in addition, the C–O vibration peak of carboxylic acids was observed at 1,239  $\text{cm}^{-1}$ , and the peaks between 400–600  $\text{cm}^{-1}$  indicate M–O vibrations.

After loading the biosorbent with Cd(II) and Pb(II) ions, shifts were found in the peaks in the spectra (Fig. 1b and c). This is interpreted as the interaction between the functional

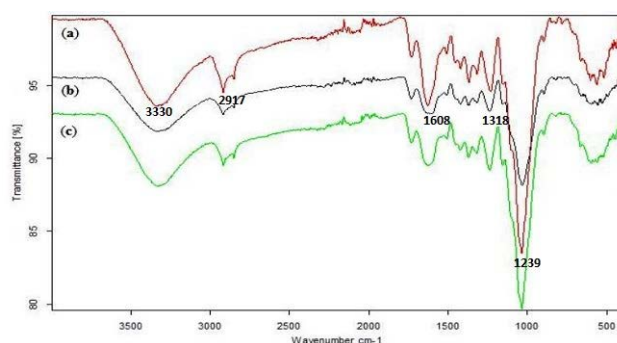


Fig. 1. FT-IR spectra of *Paliurus spina-christi* Mill. (a) unloaded, (b) Cd(II)-loaded and (c) Pb(II)-loaded.

groups on the surface of the biomass and the Cd(II) and Pb(II) ions.

The microstructures of unloaded and heavy metal (Pb(II) and Cd(II)) loaded biomass were examined by SEM and EDX spectroscopy. The scanning electron micrographs and the EDX spectra are shown in Fig. 2. Before the biosorption, the biosorbent exhibited a rough surface morphology with irregular shape and pore size that suggests a high biosorption capacity (Fig. 2a). After the biosorption process, decreases in the porosity of the biosorbent surface due to the binding of metal ions could be seen in the SEM images of the loaded biosorbents (Fig. 2b and c). Also, characteristic Pb(II) and Cd(II) ions peaks in EDX spectra confirmed that the sorption occurred on the surface of the biosorbents.

The BET surface area of *Paliurus spina-christi* Mill. was determined to be  $13.97 \text{ m}^2 \text{ g}^{-1}$ . The surface areas of the biosorbents after coating the surface with Pb(II) and Cd(II) ions were measured as  $8.93$  and  $7.11 \text{ m}^2 \text{ g}^{-1}$ , respectively. This decrease in the specific surface areas evaluated according to the multi-point BET method was due to the placement of metal ions in the pores. In addition, similar results have been reported for different biosorbents in previous studies;  $2.64 \text{ m}^2 \text{ g}^{-1}$  for *Sambucus nigra* L. [31],  $31.32 \text{ m}^2 \text{ g}^{-1}$  for *Phoenix dactylifera* [32],  $6.13 \text{ m}^2 \text{ g}^{-1}$  for date palm empty fruit bunch [33],  $0.679 \text{ m}^2 \text{ g}^{-1}$  for Pristine durian peels [34].

The zeta potential value is related to the stability of colloidal dispersions while explaining the interaction forces between particles. When suspended particles have low density and large negative/positive zeta potential, they repel each other, so the system is stable, and resistance to aggregation occurs [29]. For zeta potential measurements, samples were prepared to be  $1 \text{ mg mL}^{-1}$ , and the measurements were repeated ten times. The zeta potential of *Paliurus spina-christi* Mill. was measured as  $-30.70 \pm 0.80 \text{ mV}$ , while the zeta potential after Cd(II) and Pb(II) ions biosorption onto the biosorbent was  $-25.20 \pm 1.56$  and  $-15.93 \pm 1.20 \text{ mV}$ , respectively. These results indicate that heavy metals are successfully attached to the biosorbent surface, and therefore, the surface charge of the biosorbent increases.

## 3.2. Biosorption experiments

### 3.2.1. Effect of pH

One of the most important parameters in the biosorption process is the pH of the aqueous solution. pH affects

the solubility of metal ions and the concentration of the counter ions' binding to functional groups on the biosorbent surface. In addition, the activity of functional groups in biosorbent and the competition of metal ions also depend on pH. A protonated biosorbent releases hydronium ions during the biosorption of metals, which decreases the pH of the solution. These changes in pH are rapid in the initial period, when most of the biosorption occurs in the initial step, then they gradually reach equilibrium [35]. Therefore pH should be controlled throughout the process. Biosorption of Pb(II) and Cd(II) ions onto *Paliurus spina-christi* Mill. was investigated in the 1.5–6.0 pH range (Fig. 3). The removal efficiency of both metal ions by the biosorbent increased with the increase in the solution pH from 1.5 to 6.0. Due to the high hydronium ion concentration in the solution at low pH values, the binding sites on the biosorbent surface reach saturation. Therefore, metal removal is less for these pH values, while metal removal increases with increased pH [36]. Fig. 3 indicates that the biosorption yield for Pb(II) ions regularly increases, up to pH values of 5.5, and remains constant for pH values of 5.5–6.0. Maximum biosorption yield was determined to be 94% for a pH value of 5.5. It was observed that the biosorption yield of Cd(II) ions onto *Paliurus spina-christi* Mill. increased from 8% to 68% for pH values between 1.5 to 5.0, respectively. Therefore, the optimum pH for the removal of Cd(II) ions was determined to be 5.0.

### 3.2.2. Effect of biosorbent dosage

As in previous studies, the biosorption efficiency is directly related to the amount of biosorbent, in other words, with the increase in the amount of biosorbent, the biosorption efficiency also increases [37]. Increasing the dose of biosorbent more than the optimum amount causes agglomeration of the biosorbent, thus reducing the biosorption capacity. In addition, agglomeration reduces the active sites used for metal biosorption. According to Fig. 4, the steep slope at the beginning of the process is due to the fact that metal ions can easily reach the active sites on the biosorbent surface. The biosorption efficiency continues at a low rate until the optimum amounts, and after these amounts, the biosorption efficiency decreases with the increase in the viscosity of the solution [38]. Biosorption experiments of Pb(II) and Cd(II) ions onto *Paliurus spina-christi* Mill. were carried out to determine the minimum biosorbent dosages required for maximum removal of both metals. Results demonstrate

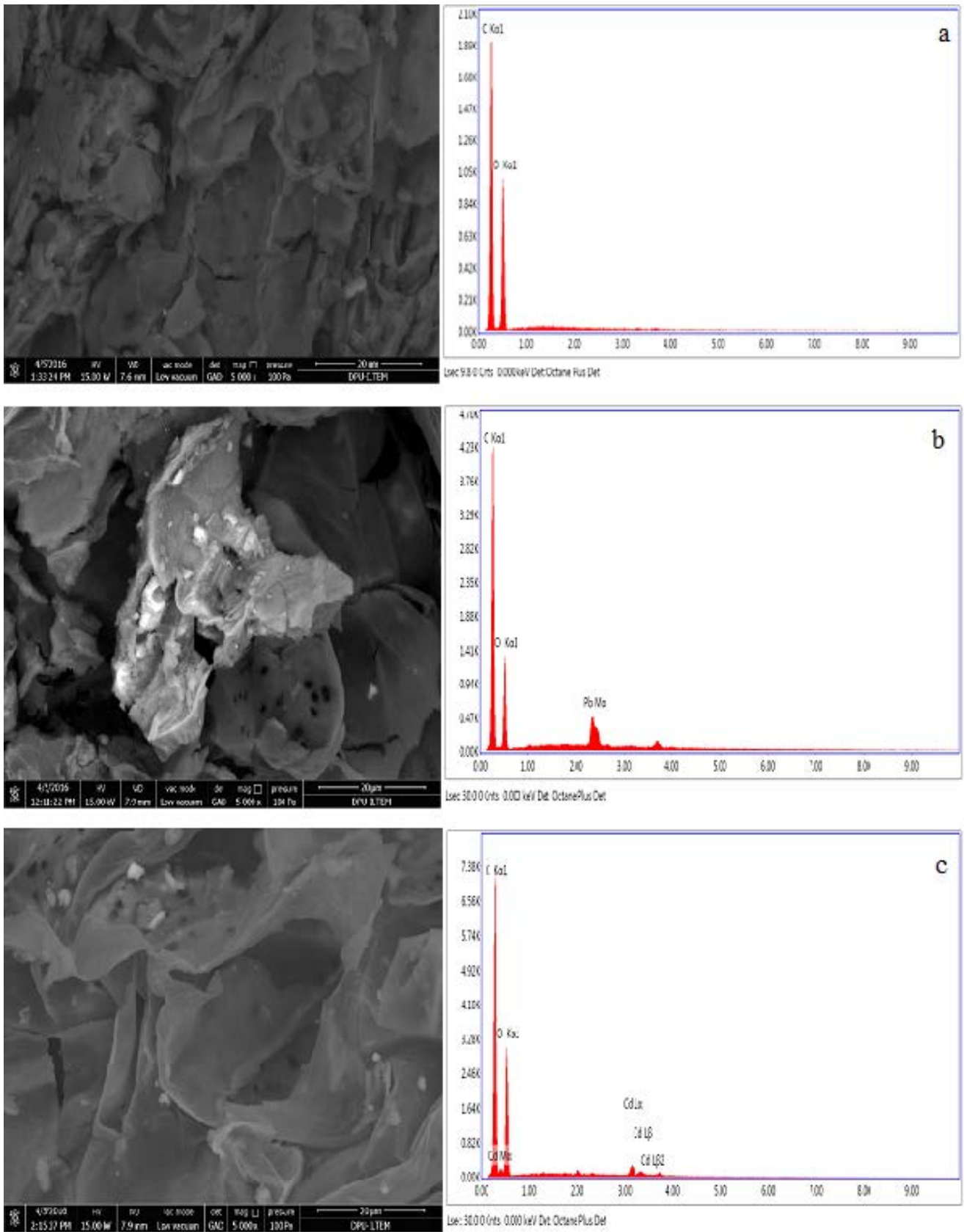


Fig. 2. SEM images and EDX spectrums of *Paliurus spina-christi* Mill. (a) unloaded, (b) Pb(II)-loaded and (c) Cd(II)-loaded.

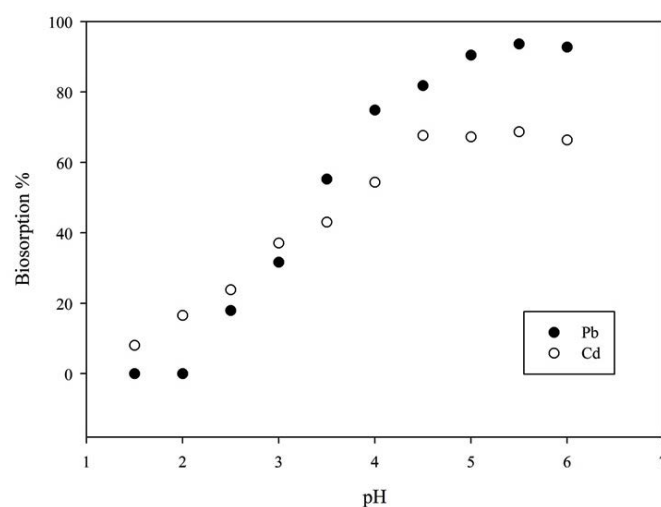


Fig. 3. Effect of solution pH on the biosorption yields of Pb(II) and Cd(II) ions at room temperature.

that the highest biosorption yields of Pb(II) and Cd(II) ions were achieved at the biosorbents doses of 2.0 and 6.0 g L<sup>-1</sup>, respectively (Fig. 4). As such, these dosages were employed for the rest of experiments.

### 3.2.3. Effect of contact time

At the beginning of the biosorption, there are many active binding sites on the surface of the biosorbent. However, as the biosorption process progresses, the surface of the biosorbent becomes saturated with metal cations and as a result of repulsive forces between the sorbent surface and the sorbate, uptake capacity decreases and process reaches to an equilibrium [39]. At equilibrium, the rate of biosorption and desorption will be equal to each other, and therefore, more biosorbate binding is not possible. Determination of the equilibrium time is important in optimizing biosorption processes [40,41]. There are three parts in the time-% biosorption graph: in the first part, the short initial period, the biosorption process is rapid. In the second part, biosorption continues at a low rate due to the empty active sites, and in the third part, the rate of biosorption slows down because the active sites are occupied [38,42]. Fig. 5a and b illustrate the effect of contact time on the removal of Pb(II) and Cd(II) ions. In the removal of Pb(II) ions, biosorption occurs rapidly and reaches equilibrium within 50 min. The contact time for all temperatures was found to be 50 min, while the biosorption yield reached 86% at 20°C and 92% at 40°C. In Cd(II) biosorption, the equilibrium time for all temperatures was determined to be 60 min. Also, it was found that the biosorption yield increased with temperature from 88% (at 20°C) to 93% (at 40°C).

### 3.2.4. Kinetic studies

Kinetic studies provide information about the rate of biosorption, equilibrium time, and the rate-limiting stages of the biosorption process [43]. Because the biosorption rate affects the solid-liquid interface, the contact time of the biosorbate is essential. In addition, the parameters calculated

from the obtained data provide information about the designing and modelling of the biosorption process. In this study, two conventional kinetic models (pseudo-first-order and pseudo-second-order) were used to describe the Pb(II) and Cd(II) ions' biosorption process onto *Paliurus spina-christi* Mill.

#### 3.2.4.1. Pseudo-first-order kinetic model

The pseudo-first-order kinetic model is not suitable for estimating the kinetics of the biosorption process, but it predicts the onset of the reaction well [44]. The first kinetic model for adsorption from an aqueous solution is the pseudo-first-order Lagergren equation. The linearized form of the pseudo-first-order rate equation is given in Eq. (3) [45].

$$\ln(q_e - q_t) = \ln q_e - k_1 t \quad (3)$$

where  $q_e$  and  $q_t$  (mg g<sup>-1</sup>) are the amounts of biosorption capacity at equilibrium and at time  $t$  (min), respectively;  $k_1$  (min<sup>-1</sup>) is the pseudo-first-order rate constant.

#### 3.2.4.2. Pseudo-second-order kinetic model

The pseudo-second-order kinetic model, which covers the reaction kinetics for all processing times, is based on solid-phase biosorption [44]. The pseudo-second-order kinetic model is known to be successfully applied in systems in which the rate-controlling step is chemisorption [36,46]. The linear model equation is provided in Eq. (4).

$$\frac{t}{q_t} = \frac{1}{k_2 q_2^2} + \frac{1}{q_2} t \quad (4)$$

where  $k_2$  (g mg<sup>-1</sup> min<sup>-1</sup>) is the pseudo-second-order rate constant. The graphs plotted for the second-order kinetic model for the biosorption of Pb(II) and Cd(II) ions are shown in Fig. 6a and b, respectively. The parameters calculated from

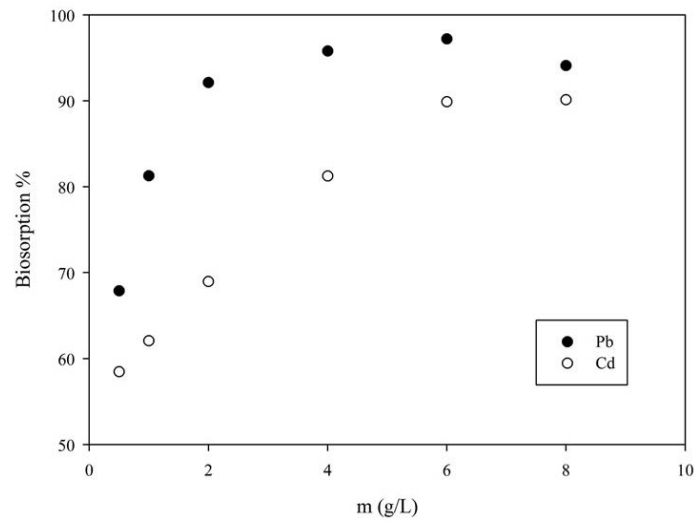


Fig. 4. Effect of biosorbent dosage on the biosorption yields of Pb(II) and Cd(II) ions at room temperature.

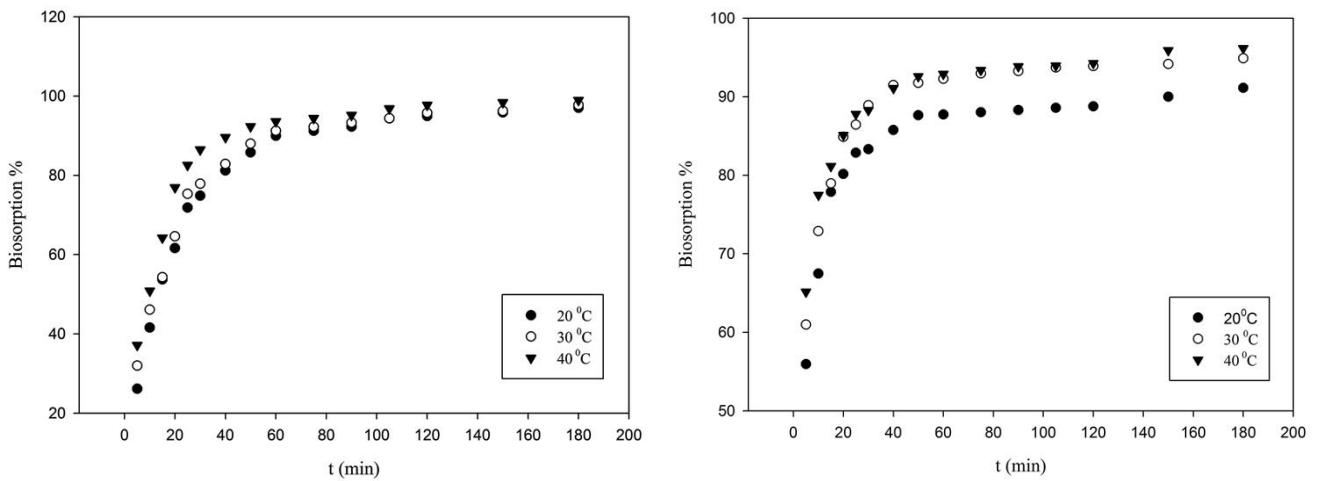


Fig. 5. Effect of contact time on the biosorption of (a) Pb(II) and (b) Cd(II) ions onto *Paliurus spina-christi* Mill. at various temperatures.

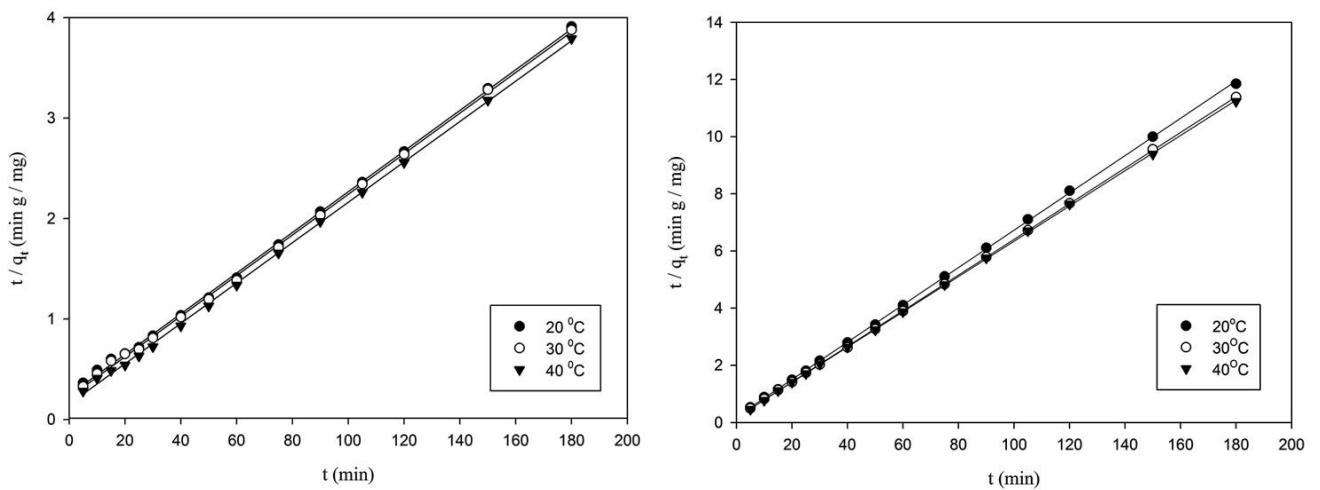


Fig. 6. Pseudo-second-order kinetic model for the biosorption of (a) Pb(II) and (b) Cd(II) ions onto *Paliurus spina-christi* Mill. at various temperatures.



the graphs are listed in Table 1. It was determined from the table that the biosorption process of both metal ions fits a pseudo-second-order kinetic model due to the high  $r_2^2$  (0.999) value. For both metals, rate constants ( $k_2$ ) were found to be slightly increased with temperature. These results indicate the acceptability of the pseudo-second-order model to explain the biosorption mechanism of Pb(II) and Cd(II) ions onto *Paliurus spina-christi* Mill.

### 3.2.5. Biosorption isotherm parameters

Biosorption isotherms are used to determine the relationship between the concentration of metal ions remaining in the solution and biosorbed on the biosorbent surface, at a constant temperature. The data from the isotherms provides information about the adsorption capacity of the biosorbent. Langmuir and Freundlich isotherms were used to express the experimental data.

#### 3.2.5.1. Langmuir model

The assumptions of Langmuir isotherm, which is known as the most common isotherm model, are as follows: (1) homogeneous monolayer biosorption occurs on the surface of the biosorbent having a certain active region, (2) no more biosorption occurs as the active sites are occupied, (3) the uptake capacity of the biosorbent is limited, (4) intermolecular attractive forces decrease with increasing distance between biosorbent and metals, (5) the energy of biosorption is constant, (6) there is no interaction between biosorbed molecules, (7) the biosorption process is reversible [36,43]. The equation for Langmuir model is frequently given as in Langmuir (1918) [47]:

$$\frac{C_e}{q_e} = \frac{1}{(q_{\max} K_L)} + \frac{C_e}{q_{\max}} \quad (5)$$

where  $C_e$  is the equilibrium concentration of Pb(II) and Cd(II) ions ( $\text{mg L}^{-1}$ ) in the solutions,  $q_e$  is the amount of Pb(II) and Cd(II) ions biosorbed onto per unit mass of *Paliurus spina-christi* Mill.,  $K_L$  is the Langmuir constant related to the energy of biosorption ( $\text{L mg}^{-1}$ ) and  $q_{\max}$  is the maximum monolayer biosorption capacity of *Paliurus spina-christi* Mill. ( $\text{mg g}^{-1}$ ).

The Langmuir isotherm also has a dimensionless separation factor ( $R_L$ ), which gives an idea of the type of biosorption isotherm, and  $R_L$  is expressed in Eq. (6)

$$R_L = \frac{1}{1 + K_L C_0} \quad (6)$$

where  $C_0$  is the initial concentration of Pb(II) and Cd(II) ions ( $\text{mg L}^{-1}$ ) and the value of  $R_L$  represents the structure of isotherms to be either favorable ( $0 < R_L < 1$ ), unfavorable ( $R_L > 1$ ), linear ( $R_L = 1$ ) or irreversible ( $R_L = 0$ ) [48].

#### 3.2.5.2. Freundlich model

According to Freundlich, the biosorption sites on the biosorbent surface are of different species and are heterogeneous. This model can be applied to systems fitted for multilayer biosorption [49]. For an amorphous biosorbent, the Freundlich model is another form of the Langmuir isotherm model. The biosorption yield represents the amount of biosorbate bound to all active sites on the surface of the biosorbent. The Freundlich model is expressed by the following equation:

$$\ln q_e = \ln K_F + \frac{1}{n} \ln C_e \quad (7)$$

where  $K_F$  ( $\text{L g}^{-1}$ ) and  $n$  (dimensionless) represent the Freundlich isotherm constants.  $n$  is a constant that provides information on the suitability of the biosorption process. Adsorption is suitable when  $n > 1$ ; in this case, new biosorption centers are formed and the adsorption capacity increases. If the value of  $n$  is equal to 1, the biosorption process is linear. When  $n < 1$ , biosorption is unsuitable. Biosorption capacity decreases because the bonds formed in the biosorption are weak [50]. Fig. 7a and b show the Langmuir isotherms of Pb(II) and Cd(II) ions, respectively. The parameters calculated from the Langmuir and Freundlich (figure not shown) isotherms are listed in Table 2. The table shows that the correlation coefficient value ( $r_1^2 = 0.999$ ) of the Langmuir isotherm model is higher than the Freundlich model for both ions. Therefore, the biosorption of the metal ions is carried out in a monolayer on the homogeneous surface of *Paliurus spina-christi* Mill. and the interaction between the ions is insignificant. The maximum biosorption capacity for Pb(II) and Cd(II) ions were found to be 231.7 and 36.84  $\text{mg g}^{-1}$  at 40°C, respectively. Dimensionless separation factor ( $R_L$ ) showed that Pb(II) and Cd(II) ions biosorption onto *Paliurus spina-christi* Mill. were favorable. In the study reported by

Table 1  
Kinetic parameters for the biosorption Pb(II) and Cd(II) ions by *Paliurus spina-christi* Mill. at various temperatures

Metal ion	Pseudo-first-order				Pseudo-second-order		
	$T$ (°C)	$k_1$ ( $\text{min}^{-1}$ )	$q_e$ ( $\text{mg g}^{-1}$ )	$r_1^2$	$k_2$ ( $\text{g mg}^{-1} \text{min}^{-1}$ )	$q_e$ ( $\text{mg g}^{-1}$ )	$r_2^2$
Pb(II)	20	$3.00 \times 10^{-2}$	12.60	0.821	$1.70 \times 10^{-3}$	49.42	0.999
	30	$3.00 \times 10^{-2}$	10.87	0.786	$1.90 \times 10^{-3}$	49.47	0.999
	40	$2.61 \times 10^{-2}$	7.665	0.737	$2.70 \times 10^{-3}$	49.74	0.999
Cd(II)	20	$1.29 \times 10^{-2}$	1.013	0.201	$2.08 \times 10^{-2}$	15.33	0.999
	30	$9.20 \times 10^{-3}$	1.043	0.172	$2.15 \times 10^{-2}$	16.03	0.999
	40	$9.90 \times 10^{-2}$	1.064	0.212	$2.27 \times 10^{-2}$	16.21	0.999



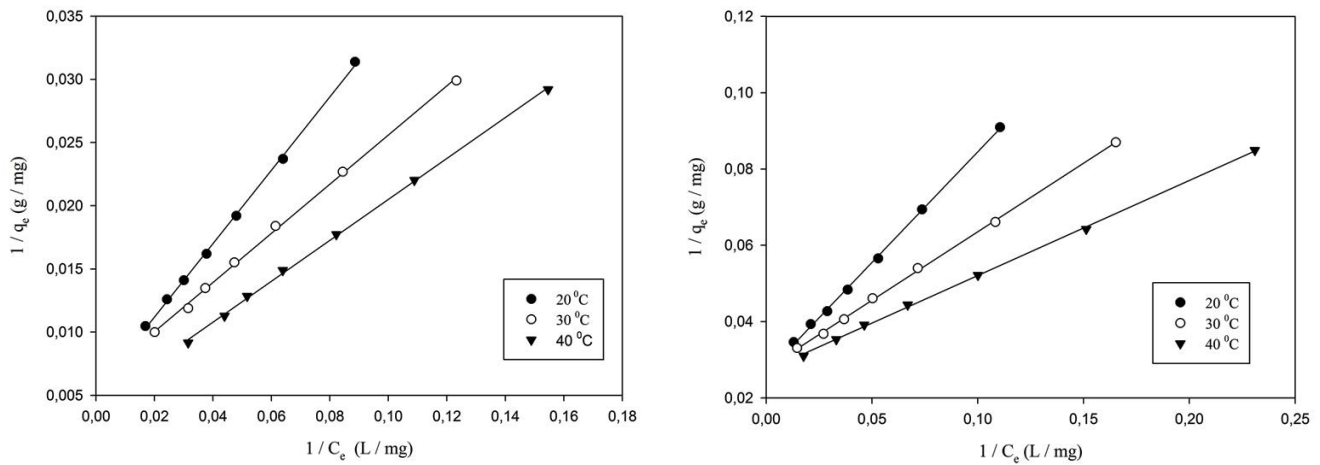


Fig. 7. Langmuir isotherms for the biosorption of (a) Pb(II) and (b) Cd(II) ions onto *Paliurus spina-christi* Mill.

Table 2

Isotherm model parameters for the biosorption of Pb(II) and Cd(II) ions by *Paliurus spina-christi* Mill.

Metal ion	Langmuir					Freundlich		
	$T$ (°C)	$K_L$ (L mg <sup>-1</sup> )	$q_{max}$ (mg g <sup>-1</sup> )	$r_L^2$	$R_L$	$K_F$ (L g <sup>-1</sup> )	$n$	$r_F^2$
Pb(II)	20	$1.87 \times 10^{-2}$	185.5	0.999	0.177	3.80	1.51	0.990
	30	$2.16 \times 10^{-2}$	216.6	0.998	0.156	7.46	1.40	0.996
	40	$2.67 \times 10^{-2}$	231.7	0.999	0.130	8.96	1.37	0.998
Cd(II)	20	$4.37 \times 10^{-2}$	35.83	0.999	0.0840	4.07	2.20	0.974
	30	$7.70 \times 10^{-2}$	36.20	0.999	0.0494	5.88	2.50	0.958
	40	$1.09 \times 10^{-1}$	36.84	0.999	0.0354	7.38	2.57	0.961

Babalola et al. [51], the biosorption capacity of lead(II) biosorption onto *Delonix regia* pods and *Delonix regia* leaves was found to be 30.27 and 27.60 mg g<sup>-1</sup>, respectively. Similarly, researchers [52] used Dried cactus cladodes as biosorbent and reported Cd(II) and Pb(II) biosorption capacities as 30.42 and 98.62 mg g<sup>-1</sup>, respectively. Although it is difficult to compare the obtained biosorption capacity to previously published studies due to differences in experimental conditions, the suggested biosorbent in this study exhibited satisfactory heavy metal biosorption.

### 3.3. Discussion on biosorption mechanism

In the case of a biosorption process, the liquid phase (dissolved species) is attracted to the solid phase (biosorbent) and is bound there by different mechanisms. This process takes place until an equilibrium is established between the phases. In addition, the degree of affinity between the adsorbate and the biosorbent determines the distribution between the solid and liquid phases. The equilibrium distribution of solute is an important feature of biosorption systems and is a decisive factor in determining the capacity of a specific system. While the mechanism of biosorption differs according to the type of biosorbent and the contaminant present in the sample, the complexity of the biomass may cause several mechanisms to be present simultaneously [53].

The biomass surface consists of polysaccharides, proteins, lipids, hydrocarbons, sugars, and other organic compounds that present a wide variety of functional groups such as –OH, –NH, –COOH, –CO. Consequently, the biosorption properties of biomass are determined by the composition of the cell wall, particularly the density of functional groups involved in the binding of metal cations. Proposed uptake mechanism of biosorbent is exhibited in Fig. 8 [54].

Biosorption kinetics and isotherms are essential in explaining the biosorption mechanism. The kinetic models evaluated in this study reflected that the pseudo-second-order kinetic model for both Pb(II) and Cd(II) biosorption was optimal, suggesting that the rate-controlling mechanism for biosorption is chemisorption [55]. In addition, the increase in equilibrium biosorption capacities with increasing temperature showed that the process occurred endothermically. From the equilibrium data obtained from Pb(II) and Cd(II) biosorption, it was found that the biosorption was consistent with the Langmuir isotherm model. In addition, the fact that the  $R_L$  values, which is an important parameter of the Langmuir isotherm model, which defines the suitability of biosorption, are much smaller than 1, proves that the biosorption of Pb(II) and Cd(II) ions on *Paliurus spina-christi* Mill. is extremely suitable. The fact that the Freundlich constant  $1/n$  was between 0 and 1 showed that the process was desirable. In addition, it can

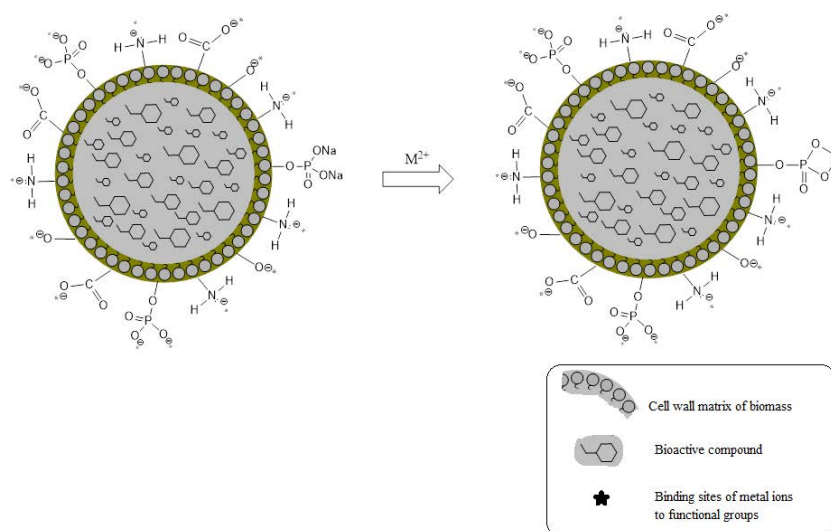


Fig. 8. Binding of metal ions to the functional groups present on the surface of biomass.

be interpreted that biomass has a significant potential for the efficient removal of metals from wastewater containing Pb(II) and Cd(II).

### 3.4. Desorption studies

Desorption yield is an important parameter for the biomaterial to be evaluated in industrial applications as well as the biosorption yield. The high regeneration ability makes the biomaterial cost-effective and more valuable in large-scale treatments. 0.1 M HCl and HNO<sub>3</sub> were used as desorption agents. In the first cycle, the whole amount of biosorbed Pb(II) ions were removed with both of the agents as the removal percentage of Cd(II) ions was nearly between 74%–70% with both HCl and HNO<sub>3</sub>. As can be seen from Figs. 9 and 10, in the third cycle, desorption yield decreased to 87% and 63% with HCl and 77% and 60% with HNO<sub>3</sub> at the removal of Pb(II) and Cd(II) ions, respectively. It is

clear that HCl is more proper for this desorption process. Since lead has a smaller hydrated radius, the biosorbent releases Pb ions more easily than Cd ions [53]. Because also the decrease in the percentages of biosorption increased after the third cycle due to the degeneration of biosorbent structure, experiments were not continued for further cycles.

### 3.5. Application in simulated wastewater

To determine the real performance of biosorbent, an application in simulated wastewater was evaluated. Many other metallic salts were dissolved with Pb(II) and Cd(II) ions to prepare the wastewater, as described in section 2.5. Biosorption yield in simulated wastewater was obtained as 90% and 60% for Pb(II) and Cd(II) ions, respectively. It was seen that biosorption capacity wasn't influenced by the presence of other metallic ions, anions, and organic constituents at the Pb(II) ions removal. It can

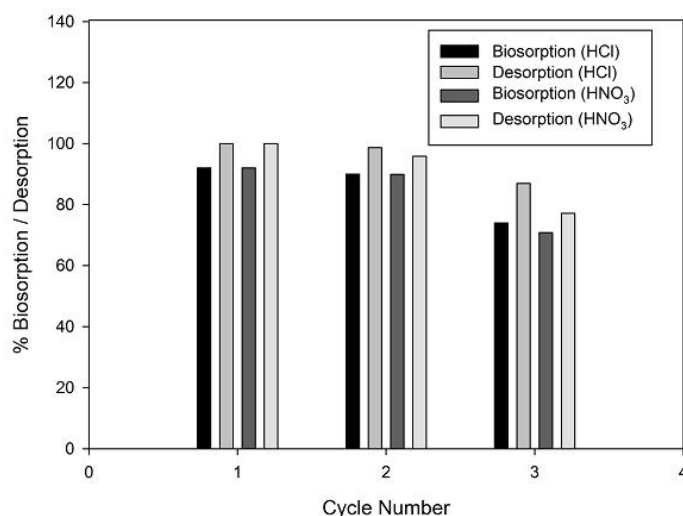


Fig. 9. Biosorption and desorption yield of *Paliurus spina-christi* Mill. for Pb(II) ions by consecutive adsorption-desorption cycles.

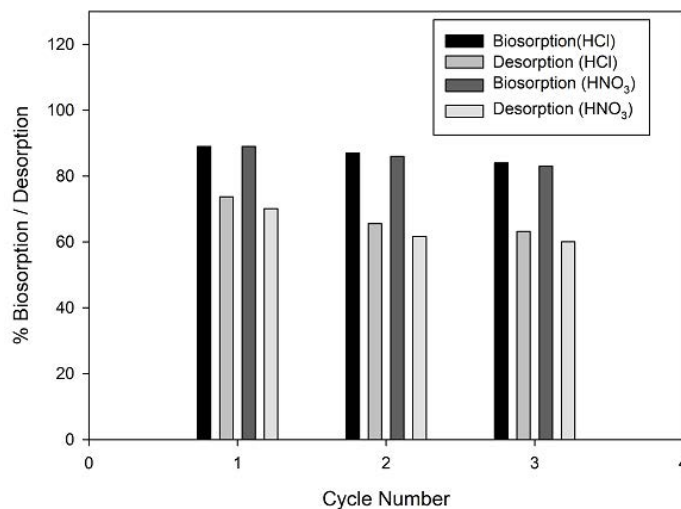


Fig. 10. Biosorption and desorption yield of *Paliurus spina-christi* Mill. for Cd(II) ions by consecutive adsorption–desorption cycles.

be said that the biosorbent is selective for Pb(II) ions. The capacity of biosorbent for Cd(II) ions was 89% with synthetic cadmium solution, but its yield decreased to 60% when studied with simulated wastewater. It is clear that matrix effect is more important in cadmium biosorption.

#### 4. Conclusions

In this study, removal of heavy metals using agricultural biomass was investigated. These kinds of biosorbents, which are highly effective for the removal of metal ions, are also economical and environmentally friendly. The effects of the biosorption process parameters such as biosorbent dosage, pH, contact time and temperature were examined for the Pb(II) and Cd(II) ions removal process. Furthermore, possible interactions between the biosorbent and metal ions and surface characterization of the biosorbent have been investigated using various methods (FT-IR, SEM-EDX, Zeta potential, BET Analysis). Optimum pH for Pb(II) and Cd(II) ions were determined as 5.5 and 5.0, respectively. The studies carried out at these pHs showed that the biosorption equilibrium was established within 40–60 min. Also, the experimental kinetic data was found to follow the pseudo-second-order model for both metal ions. It was determined from the equilibrium data that the biosorption process conforms to the Langmuir isotherm and that the surface of the biosorbent is coated by a monolayer of metal ions. The maximum monolayer biosorption capacity for Pb(II) and Cd(II) ions were obtained as 231.7 and 36.84 mg g<sup>-1</sup> at 40°C, respectively. In consecutive biosorption–desorption cycles, 0.1 M HCl is determined as the most effective desorption agent providing over 85% and 63% desorption yield at the third cycle for Pb(II) and Cd(II) ions respectively. Real sample application is performed by preparing simulated wastewater. Experiments showed that biosorbent exhibited the same Pb(II) biosorption capacity (90%) provided with the synthetic solutions while there is a significant decrease from 89% to 60% at the biosorption capacity of Cd(II) ions at synthetic and real applications. From the results, it can be said that biosorbent is more

selective to Pb(II) ions. In conclusion, the findings of our study indicate that the proposed biosorbent is an effective, low cost, and environmentally friendly biomass to be used for the removal of Pb(II) and Cd(II) ions for a series of biosorption–desorption cycles.

#### Disclosure statement

The authors have no conflict of interest for the present study.

#### References

- [1] N. Feng, X. Guo, S. Liang, Y. Zhu, J. Liu, Biosorption of heavy metals from aqueous solutions by chemically modified orange peel, *J. Hazard. Mater.*, 185 (2011) 49–54.
- [2] M.L. Nguyen, C. Huang, R.S. Juang, Synergistic biosorption between phenol and nickel(II) from binary mixtures on chemically and biologically modified chitosan beads, *Chem. Eng. J.*, 286 (2016) 68–75.
- [3] G.L. Dotto, L. Sellaoui, E.C. Lima, A. Ben Lamine, Physicochemical and thermodynamic investigation of Ni(II) biosorption on various materials using the statistical physics modeling, *J. Mol. Liq.*, 220 (2016) 129–135.
- [4] N.A. Bingöl, F. Özmal, B. Akın, Phytoremediation and biosorption potential of *Lythrum salicaria* L. For nickel removal from aqueous solutions, *Pol. J. Environ. Stud.*, 26 (2017) 2479–2485.
- [5] A.G. Adeniyi, J.O. Ighalo, Biosorption of pollutants by plant leaves: an empirical review, *J. Environ. Chem. Eng.*, 7 (2019) 103100, doi: 10.1016/j.jece.2019.103100.
- [6] E. Babaei, S.A. Hashemifard, Polycarbonate/copper oxide mixed matrix membrane for separation of lead and cadmium from industrial effluents, *Sep. Sci. Technol.*, 57 (2021) 619–636.
- [7] G.R. de Freitas, M.G.C. da Silva, M.G.A. Vieira, Biosorption technology for removal of toxic metals: a review of commercial biosorbents and patents, *Environ. Sci. Pollut. Res.*, 26 (2019) 19097–19118.
- [8] H. Habibi, N. Dalali, A. Ramazani, Decoration of maleic/acrylic acid onto CoFe<sub>2</sub>O<sub>4</sub> as a high-performance nanosorbent for the removal of lead(II) and cadmium(II) from environmental samples, *Sep. Sci. Technol.* 56 (2021) 2036–2046.
- [9] F.I. Anuar, T. Hadibarata, Muryanto, A. Yuniarto, D. Priyandoko, A.A. Sari, Innovative chemically modified biosorbent for removal of Procion Red, *Int. J. Technol.*, 10 (2019) 776–786.

- [10] L. Qin, L. Feng, C. Li, Z. Fan, G. Zhang, C. Shen, Q. Meng, Amination/oxidization dual-modification of waste ginkgo shells as bio-adsorbents for copper ion removal, *J. Cleaner Prod.*, 228 (2019) 112–123.
- [11] T. Shahnaz, V. Vishnu Priyan, A. Jayakumar, S. Narayanasamy, Magnetic nanocellulose from *Cyperus rotundas* grass in the absorptive removal of rare earth element cerium(III): toxicity studies and interpretation, *Chemosphere*, 287 (2022) 131912, doi: 10.1016/j.chemosphere.2021.131912.
- [12] A. Gundogdu, D. Ozdes, C. Duran, V.N. Bulut, M. Soylyak, H.B. Senturk, Biosorption of Pb(II) ions from aqueous solution by pine bark (*Pinus brutia* Ten.), *Chem. Eng. J.*, 153 (2009) 62–69.
- [13] K. Chojnacka, Biosorption and bioaccumulation – the prospects for practical applications, *Environ. Int.*, 36 (2010) 299–307.
- [14] V.B.H. Dang, H.D. Doan, T. Dang-Vu, A. Lohi, Equilibrium and kinetics of biosorption of cadmium(II) and copper(II) ions by wheat straw, *Bioresour. Technol.*, 100 (2009) 211–219.
- [15] A. Safa Özcan, S. Tunali, T. Akar, A. Özcan, Biosorption of lead(II) ions onto waste biomass of *Phaseolus vulgaris* L.: estimation of the equilibrium, kinetic and thermodynamic parameters, *Desalination*, 244 (2009) 188–198.
- [16] R. Saygili Canlidinc, O.M. Kalfa, Z. Üstündağ, Y. Erdoğan, Graphene oxide modified expanded perlite as a new sorbent for Cu(II) and Pb(II) prior to determination by high-resolution continuum source flame atomic absorption spectrometry, *Sep. Sci. Technol.*, 52 (2017) 2069–2078.
- [17] G. Yuvaraja, N. Krishnaiah, M.V. Subbaiah, A. Krishnaiah, Biosorption of Pb(II) from aqueous solution by Solanum melongena leaf powder as a low-cost biosorbent prepared from agricultural waste, *Colloids Surf.*, 114 (2014) 75–81.
- [18] V. Jayakumar, S. Govindaradjane, M. Rajasimman, Isotherm and kinetic modeling of sorption of cadmium onto a novel red algal sorbent, *Hypnea musciformis*, *Model. Earth Syst. Environ.*, 5 (2019) 793–803.
- [19] R. Bhateria, R. Dhaka, Optimization and statistical modelling of cadmium biosorption process in aqueous medium by *Aspergillus niger* using response surface methodology and principal component analysis, *Ecol. Eng.*, 135 (2019) 127–138.
- [20] World Health Organization (WHO), Cadmium in Drinking Water, WHO Press, Switzerland, 2011.
- [21] C. Schirarend, M.N. Olabi, Revision of the genus *Paliurus* Toum. ex MILL. (Rhamnaceae), *Bot. Jahrb. Syst.*, 116 (1994) 333–359.
- [22] S.E. Shahbaz, N.M. Shareef, Use of morphological and anatomical characters to delimit varieties of *Paliurus spinachristi* Mill. (Rhamnaceae), *Innovaciencia Fac. Ciencias Exactas Fisicas y Nat.*, 6 (2018) 1–14.
- [23] P.H. Davis, Flora of Turkey and the East Aegean Islands, 2, Edinburgh University Press, Edinburgh, 1967.
- [24] Ç. Ömeroglu Ay, A.S. Özcan, Y. Erdoğan, A. Özcan, Characterization of *Punica granatum* L. peels and quantitative determination of its biosorption behavior towards lead(II) ions and Acid Blue 40, *Colloids Surf.*, 100 (2012) 197–204.
- [25] M. Medić-Šarić, Ž. Males, S. Šarić, A. Brantner, Quantitative modeling of flavonoid glycosides isolated from *Paliurus spinachristi* Mill., *Croat. Chem. Acta*, 69 (1996) 1603–1616.
- [26] A. Ronchese, The constituents of *Paliurus aculeatus* Lamk (Rhamnaceae) with particular emphasis on a heteroside, *Ann. Pharm. Fr.*, 10 (1952) 676–680.
- [27] K.M. Brodowska, Natural flavonoids: classification, potential role, and application of flavonoid analogues, *Eur. J. Biol. Res.*, 7 (2017) 108–123.
- [28] L. Wulandari, B.D. Permana, N. Kristiningrum, Determination of total flavonoid content in medicinal plant leaves powder using infrared spectroscopy and chemometrics, *Indones. J. Chem.*, 20 (2020) 1044–1051.
- [29] A. El-Ansary, A. Warsy, M. Daghestani, N.M. Merghani, A. Al-Dbass, W. Bukhari, B. Al-Ojayan, E.M. Ibrahim, A.M. Al-Qahtani, R.S. Bhat, Characterization, antibacterial, and neurotoxic effect of green synthesized nanosilver using *Ziziphus spina christi* aqueous leaf extract collected from Riyadh, Saudi Arabia, *Mater. Res. Express.*, 5 (2018), doi: 10.1088/2053-1591/aaaf5f.
- [30] S. Kummara, M.B. Patil, T. Uriah, Synthesis, characterization, biocompatible and anticancer activity of green and chemically synthesized silver nanoparticles – a comparative study, *Biomed. Pharmacother.*, 84 (2016) 10–21.
- [31] T. Kalak, J. Dudczak-Hałaabuda, Y. Tachibana, R. Cierpiszewski, Effective use of elderberry (*Sambucus nigra*) pomace in biosorption processes of Fe(III) ions, *Chemosphere*, 246 (2020) 125744, doi: 10.1016/j.chemosphere.2019.125744.
- [32] K. Rambabu, A. Thanigaivelan, G. Bharath, N. Sivarajasekar, F. Banat, P.L. Show, Biosorption potential of *Phoenix dactylifera* coir wastes for toxic hexavalent chromium sequestration, *Chemosphere*, 268 (2021) 128809.
- [33] K. Rambabu, G. Bharath, F. Banat, P.L. Show, Biosorption performance of date palm empty fruit bunch wastes for toxic hexavalent chromium removal, *Environ. Res.*, 187 (2020) 109694, doi: 10.1016/j.envres.2020.109694.
- [34] M. Ngabura, S.A. Hussain, W.A.W.A. Ghani, M.S. Jami, Y.P. Tan, Utilization of renewable durian peels for biosorption of zinc from wastewater, *J. Environ. Chem. Eng.*, 6 (2018) 2528–2539.
- [35] S.H. Abbas, I. Ismail, T. Moustafa, A.H. Sulaymon, Biosorption of Heavy Metals, *Heavy Met. Sources, Toxic. Remediat. Tech.*, 2016, pp. 131–174.
- [36] S. Rangabhashiyam, P. Balasubramanian, Characteristics, performances, equilibrium and kinetic modeling aspects of heavy metal removal using algae, *Bioresour. Technol. Rep.*, 5 (2019) 261–279.
- [37] E. Nakkeeran, S. Rangabhashiyam, M.S. Giri Nandagopal, N. Selvaraju, Removal of Cr(VI) from aqueous solution using *Strychnos nux-vomica* shell as an adsorbent, *Desal. Water Treat.*, 57 (2016) 23951–23964.
- [38] A.A. Beni, A. Esmaeili, Biosorption, an efficient method for removing heavy metals from industrial effluents: a review, *Environ. Technol. Innov.*, 17 (2020) 100503, doi: 10.1016/j.eti.2019.100503.
- [39] I. Hegazy, M.E.A. Ali, E.H. Zaghlool, R. Elsheikh, Heavy metals adsorption from contaminated water using moringa seeds/olive pomace byproducts, *Appl. Water Sci.*, 11 (2021) 1–14.
- [40] M.M. Montazer-Rahmati, P. Rabbani, A. Abdolali, A.R. Keshtkar, Kinetics and equilibrium studies on biosorption of cadmium, lead, and nickel ions from aqueous solutions by intact and chemically modified brown algae, *J. Hazard. Mater.*, 185 (2011) 401–407.
- [41] M. Zaib, M.M. Athar, A. Saeed, U. Farooq, M. Salman, M.N. Makshoof, Equilibrium, kinetic and thermodynamic biosorption studies of Hg(II) on red algal biomass of porphyridium cruentum, *Green Chem. Lett. Rev.*, 9 (2016) 179–189.
- [42] F. Wang, Y. Pan, P. Cai, T. Guo, H. Xiao, Single and binary adsorption of heavy metal ions from aqueous solutions using sugarcane cellulose-based adsorbent, *Bioresour. Technol.*, 241 (2017) 482–490.
- [43] Z. Movasaghi, B. Yan, C. Niu, Adsorption of ciprofloxacin from water by pretreated oat hulls: equilibrium, kinetic, and thermodynamic studies, *Ind. Crops Prod.*, 127 (2019) 237–250.
- [44] E. Daneshvar, A. Vazirzadeh, A. Niazi, M. Sillanpää, A. Bhatnagar, A comparative study of methylene blue biosorption using different modified brown, red and green macroalgae – effect of pretreatment, *Chem. Eng. J.*, 307 (2017) 435–446.
- [45] S. Lagergren, K. Sven, Zur theorie der sogenannten adsorption gelöster stoffe, *Vetenskapsakademiens. Handl.*, 24 (1898) 1–39.
- [46] Y.S. Ho, G. McKay, Pseudo-second-order model for sorption processes, *Process Biochem.*, 34 (1999) 451–465.
- [47] I. Langmuir, The adsorption of gases on plane surfaces of glass, mica and platinum, *J. Am. Chem. Soc.*, 40 (1918) 1361–1403.
- [48] T.W. Weber, R.K. Chakravorti, Pore and solid diffusion models for fixed-bed adsorbents, *AIChE J.*, 20 (1974) 228–238.
- [49] H. Freundlich, W. Heller, The adsorption of cis- and trans-azobenzene, 61 (1939) 2228–2230.
- [50] B. Al-Duri, G. McKay, Eds., Use of Adsorbents for the Removal of Pollutants from Wastewaters, 1st ed., CRC Press, 1996, pp. 133–173.
- [51] B.M. Babalola, A.O. Babalola, H.O. Adubiaro, O.S. Ayanda, S.M. Nelana, E.B. Naidoo, Application of waste delonix regia

- Pods and leaves for the sorption of Pb(II) ions from aqueous solution: kinetic and equilibrium studies, *Water Qual. Res. J.*, 54 (2019) 278–289.
- [52] N. Barka, M. Abdennouri, M. El Makhfouk, S. Qourzal, Biosorption characteristics of cadmium and lead onto eco-friendly dried cactus (*Opuntia ficus indica*) cladodes, *J. Environ. Chem. Eng.*, 1 (2013) 144–149.
- [53] L.B. Escudero, P.Y. Quintas, R.G. Wuilloud, G.L. Dotto, Biosorption of Metals and Metalloids, In: *Green Adsorbents for Pollutant Removal*, Springer, Cham, 2018, pp. 35–86.
- [54] I. Michalak, A. Witek-Krowiak, K. Chojnacka, A. Bhatnagar, Advances in biosorption of microelements – the starting point for the production of new agrochemicals, *Rev. Inorg. Chem.*, 35 (2015) 115–133.
- [55] S. Tasrin, S. Mohamed Madhar Fazil, S. Senthilmurugan, N. Selvaraju, Facile preparation of nanocellulose embedded polypyrrole for dye removal: unary and binary process optimization and seed toxicity, *Int. J. Environ. Sci. Technol.*, 18 (2021) 365–378.